

PROCEEDINGS OF SPIE

SPIDigitalLibrary.org/conference-proceedings-of-spie

High-power, continuous-wave, scalable, single-frequency 852nm laser source for 213nm generation

Yushi Kaneda, Tsuyoshi Tago, Toshiaki Sasa, Masahiro Sasaura, Hiroaki Nakao, et al.

Yushi Kaneda, Tsuyoshi Tago, Toshiaki Sasa, Masahiro Sasaura, Hiroaki Nakao, Junji Hirohashi, Yasunori Furukawa, "High-power, continuous-wave, scalable, single-frequency 852nm laser source for 213nm generation," Proc. SPIE 10902, Nonlinear Frequency Generation and Conversion: Materials and Devices XVIII, 1090203 (4 March 2019); doi: 10.1117/12.2506231

SPIE.

Event: SPIE LASE, 2019, San Francisco, California, United States

High-power, continuous-wave, scalable, single-frequency 852nm laser source for 213nm generation

Yushi Kaneda^{*a,b}, Tsuyoshi Tago^a, Toshiaki Sasa^a, Masahiro Sasaura^a, Hiroaki Nakao^a,
Junji Hirohashi^a, and Yasunori Furukawa^a

^aOxide Corporation, 1747-1 Mukawa, Hokuto, Yamanashi 408-0302, JAPAN; ^bUniversity of Arizona, College of Optical Sciences, 1630 E University Blvd., Tucson, AZ 85721 USA

ABSTRACT

We developed a high-power, continuous-wave (CW), single-frequency 852nm laser source, for the purpose of fourth harmonic generation at 213nm. Our approach is the doubly resonant sum-frequency mixing (DRSFM) with two fiber sources. An in-house single-frequency master oscillator at 1907nm is amplified by an in-house clad-pumped amplifier to 5W, and a commercial single-frequency master oscillator at 1540nm is amplified by a commercial amplifier to 10W. The two beams are combined via a dichroic mirror to a single beam before incident on a dual-wavelength resonator, consisting of one set of dual-wavelength mirrors. The external resonator is locked to the 1907nm laser frequency, and the frequency of the 1540nm is locked to the resonator, realizing double-resonance. With a periodically-poled stoichiometric lithium tantalate in the resonator, the sum-frequency at 852nm is efficiently generated. All 3 waves are in the same polarization (e-ray), allowing the effective use of Brewster-cut device, eliminating reflection loss for all wavelengths without any antireflection coatings. With 4.6W at 1907nm and 7.7W at 1540nm incident onto the resonator, 5.2W at 852nm was generated, representing the efficiency of greater than 40%. The experimental result indicates our current setup will be more efficient with higher input powers at 1907nm. With both fiber sources at 1540nm and 1907nm being scalable in output power, the output at 852nm is also scalable. By the forth harmonic of 852nm, 0.456 W CW 213nm was generated.

Keywords: Harmonic generation and mixing, Fiber lasers, Frequency doubled lasers, Ultraviolet lasers

1. INTRODUCTION

Continuous-wave (CW) fourth-harmonic laser sources at 266nm, the fourth harmonic wavelength, are industrially deployed in a variety of applications. CW laser sources at 213nm, a natural next step at the fifth harmonic wavelength, had long been sought for. Demand for shorter wavelengths and higher output powers has been persistent, for example, for higher throughput or for higher S/N ratio in the inspection of semiconductor which keeps shrinking in size, or for the photoemission applications, where shorter wavelength (larger photon energy, 5.8eV for 213nm) allows the observation of materials with larger work function including some common subjects such as gold (5.1eV). In order to generate 213nm, conventionally the forth harmonic of 1064nm is frequency mixed with the fundamental [1]. However, this approach requires the forth harmonic at 266nm, which is already in the deep UV, to be tightly focused into the nonlinear crystal, hence limiting the operational lifetime of the crystal. Further, the output power will be limited by the availability of the fourth harmonic power. In this paper, we propose a new approach to reach 213nm in CW that is scalable to higher output powers, and demonstrate the CW output at 213nm up to 0.456W. To the best of our knowledge, this is the highest power reported for CW 213nm output.

For the objective of stably generating higher powers at 213nm, we decided to take a different approach [2]; 213nm is generated by the second harmonic generation (SHG) of 426nm in an external resonator. Besides the generated 213nm, this approach evidently gives the longest of the shortest wavelength involved in the nonlinear crystal. The 426nm can be obtained by the second harmonic of 852nm in an external resonator. To generate high-power at 852nm in single frequency, we chose the sum-frequency mixing as the scalable approach. Other laser sources emitting at 852nm such as Ti:sapphire laser would require suitable pump lasers that are even higher powers, and may not be diode lasers.

The combination of the two wavelengths for sum-mixing needs to be with available sources with scalable output powers. Among various possible combinations, we chose 1907nm from a thulium-doped fiber source and 1540nm from an erbium-doped fiber source. These fiber sources are readily scalable in single frequency beyond tens of watts [3, 4]. The 852nm

*kaneda@opt-oxide.com; phone +81-551-26-0022

can be efficiently generated by doubly-resonant sum-frequency mixing (DRSFM) in an external resonator, in which both the 1907nm and 1540nm are resonantly enhanced simultaneously [5]. Generated 852nm is subsequently converted to 213nm by cascaded external resonant doublers. The resulting output is purely continuous and in single frequency. Figure 1 shows the schematic of our approach.

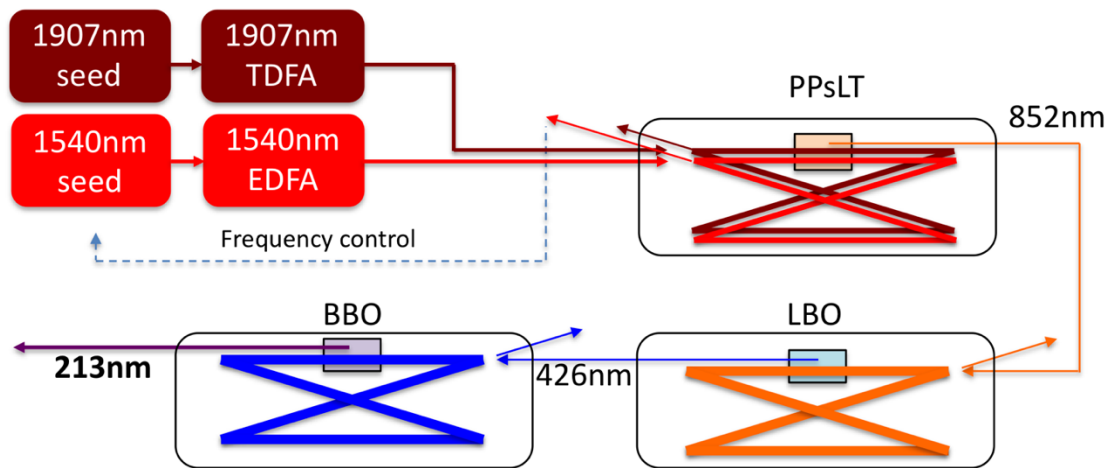


Figure 1. Schematic of the continuous-wave 213nm laser. TDFA: Thulium-Doped Fiber Amplifier, EDFA: Erbium-Doped Fiber Amplifier, PPsLT: Periodically-Poled stoichiometric Lithium Tantalate, LBO: LiB_3O_5 , BBO: $\beta\text{-BaB}_2\text{O}_4$

2. IR SOURCE AT 1907NM

The seed laser source at 1907nm is a DBR fiber laser oscillator similar to what is described in a reference [6]. A matching pair of fiber Bragg gratings was spliced to either side of a 10mm long thulium-doped single-clad fiber (Nufern SM-TSF-5/125), and pumped by a single-mode 793-nm diode laser. With 250mW of pump power, more than 40mW of single-frequency output was obtained after a dual-stage isolator. The 1907nm seed oscillator is free running and does not have the frequency tuning capability. This seed was fed into a double-clad fiber amplifier, pumped by two 9W multimode diode lasers at 793nm in forward-pumping configuration. The output end of the gain fiber is angle-cleaved for free-space output. With the maximum pump power, an output power of greater than 5W was obtained using 2m long double-clad fiber, as shown in Figure 2. The amplifier is well saturated, and no significant ASE peak is observed as shown in Figure 3. When longer fiber was used, such as 2.5m or longer, ASE builds up near 1960nm, and eventually exhibited lasing at the peak wavelength of ASE.

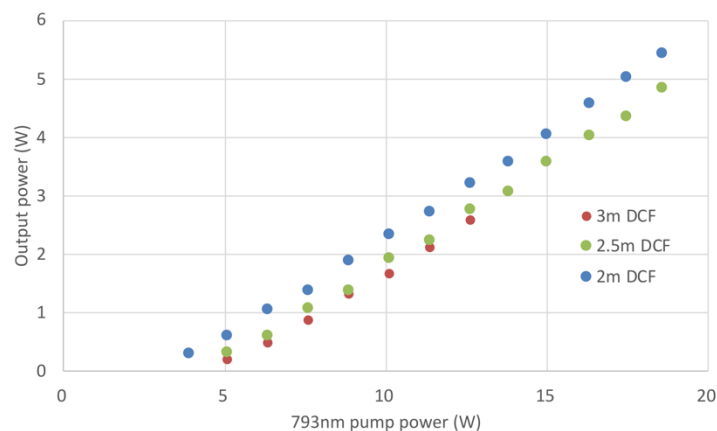


Figure 2. Output characteristics of double-clad fiber amplifier. With 3m DCF, experiment was stopped with the onset of lasing.

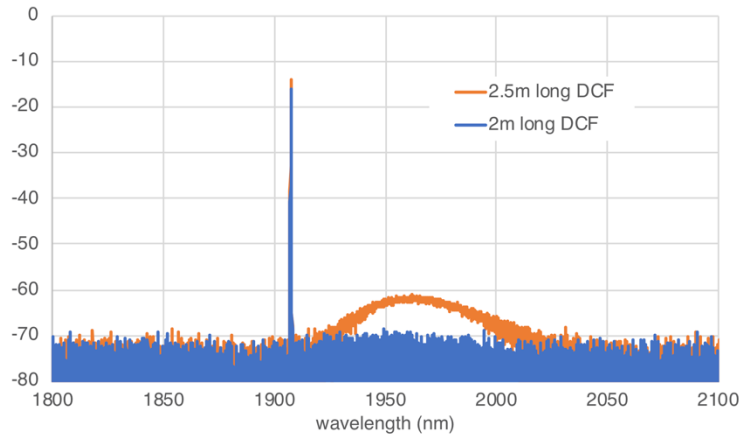


Figure 3. Spectrum of double-clad TDFA with maximum pump power with different fiber length. Seed power is 47mW.

With higher pump power or multi-stage amplifiers, the output power can be further increased. In a preliminary experiment, we have observed more than 11W output from a second stage double-clad fiber amplifier.

3. SUM-FREQUENCY MIXING AT 852NM

The 1907nm laser source described above was used in the generation of 852nm by mixing with 1540nm laser source. The 1540nm source consists of a commercial single frequency fiber oscillator (NKT Photonics) and commercial erbium-doped fiber amplifier (IPG Photonics) with maximum output power of 10W. The 1540nm oscillator has the fast frequency control capability. The output from the two fiber sources are combined with a dichroic mirror, after individually modulated in phase at different frequencies for Pound-Drever-Hall locking. This configuration was chosen for the maximum flexibility. In the experiment, the reflection from the sum-frequency resonator is separated by wavelength and 2 photodetectors are used for each wavelength. This could be simplified by using one photodetector and detecting the phase at different phase modulation frequency or modulate the phase after combining with dichroic mirror and detect with two different photodetectors.

The DRSFM cavity consists of one set of mirrors, 3 dual-wavelength high reflectors (dual-HRs) and a dual-wavelength input coupler, ensuring the modes at two different wavelengths overlap in the nonlinear crystal, with one of the dual-HRs mounted on a PZT. The dual-wavelength input coupler has the reflectivity of 96% at 1907nm and 98% at 1540nm. A Brewster-cut, 1.5mm long MgO-doped periodically-poled stoichiometric lithium tantalate (PPsLT) device, poled at $25.37\mu\text{m}$ for the first order quasi-phasematching for SFM, is placed at the waist of the cavity. As all the wavelengths are in the same polarization, the Brewster-cut device can maintain low loss at all the wavelengths involved, including the generated 852nm at the sum frequency, without any antireflection coatings which can be difficult to achieve low reflectivity at all three wavelengths. The generated 852nm is outcoupled through one of the dual-HR mirrors. The resonator mode has the waist at the PPsLT device with radii of $83\mu\text{m} \times 37\mu\text{m}$ at 1907nm and $75\mu\text{m} \times 33\mu\text{m}$ at 1540nm, respectively. The normalized conversion efficiency is estimated to be $0.5 \times 10^{-4} \text{ W}^{-1}$. With longer PPsLT device, higher normalized conversion efficiency is feasible. The cavity is locked to the free-running 1907nm by controlling the PZT, and the frequency of the 1540nm is locked to the cavity, hence realizing simultaneous resonance of two wavelengths.

Figure 4 shows the oscilloscope observation of the DRSFM experiment. Oscilloscope screenshots of 3 different situations are stitched together. In 3 channels of the oscilloscope, the transmission signal from the resonator, reflection from the resonator at different wavelength are displayed. In section I, the resonator length is scanned with the PZT and the frequency of the 1540nm is also scanned, showing the resonance at different wavelength at different position of the PZT. In section II, the PZT is locked to the 1907nm frequency and 1540nm frequency still scanned. In this situation, the floor of the transmission rises to the 1907nm peak, and the reflection at 1907nm drops. The 1540nm reflection dip becomes deeper, and the reflection at 1907nm further drops when the 1540nm frequency comes into resonance. This is because of the better impedance matching condition of the resonator by the depletion of either wavelengths from the sum-frequency process. In section III, the 1540nm frequency is locked to the resonator, so that the two wavelengths both resonantly enhanced in the cavity, efficiently generating at the sum frequency.

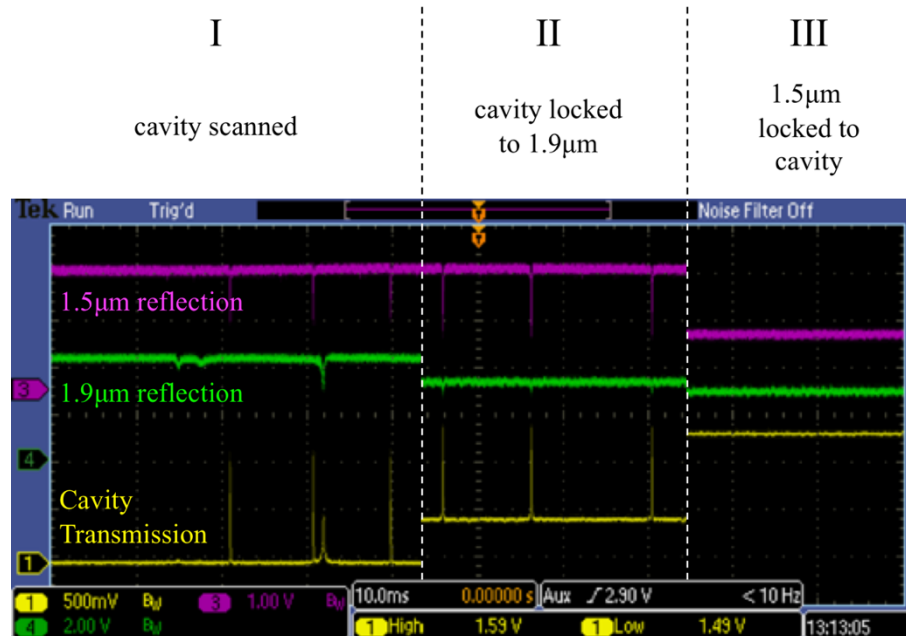


Figure 4. Observation of DRSFM experiment on an oscilloscope, showing the transmission from one of the HR mirrors, reflection at 1907nm and 1540nm. 3 screenshots from different situations are stitched together; I, cavity and 1540nm frequency are both scanned, II, cavity is locked to the 1907nm and 1540nm frequency is scanned, III, 1540nm frequency is locked to the cavity, realizing simultaneous resonance of two wavelength.

Figure 5 shows the input-output characteristics of DRSFM at 852nm with different 1907nm input powers. With the maximum available input from two fiber sources, 4.6W at 1907nm and 7.7W at 1540nm incident onto the resonator, a maximum output power of 5.2W of 852nm was observed. The total input power at both 1907nm and 1540nm is 12.3W, representing a conversion efficiency of 41%. We estimate the circulating powers at 1907nm and 1540nm are approximately 200W and 600W, respectively.

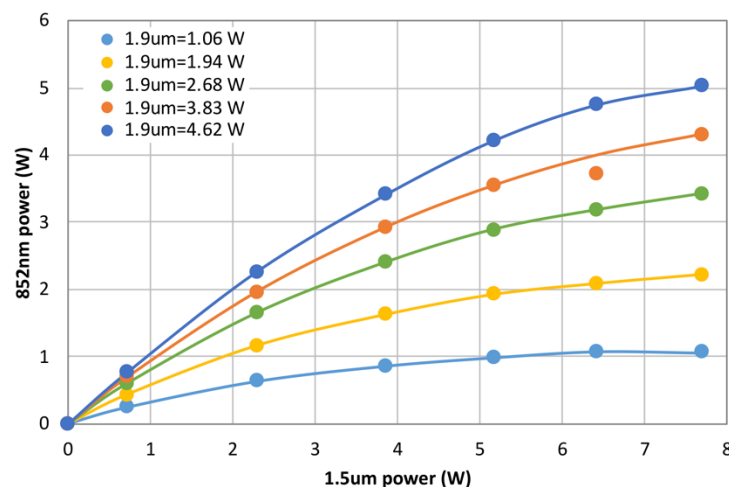


Figure 5. Input-output characteristics of DRSFM at 852nm.

Figure 6 shows the conversion efficiency from the total IR power to 852nm power for the data shown in Figure 5. For each 1907nm input power, the conversion efficiency reaches its maximum and slowly lowers with increasing 1540nm power. The 1540nm power for the maximum efficiency increases with the higher 1907nm input power, with the maximum also increasing. With the highest 1907nm input power available for the experiment, the maximum efficiency was 43%. Therefore, higher input powers at 1907nm will enable higher efficiency, and higher output powers at 852nm will be

possible. Further, with longer device of PPsLT than the present experiment and revised resonator parameters such as waist size of the resonator mode and input coupling at both 1907nm and 1540nm, the 852nm output power is scalable to much higher powers.

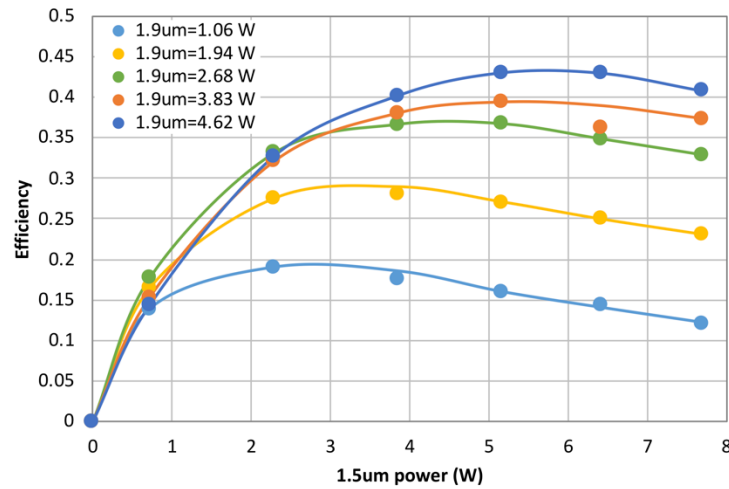


Figure 6. DRSFM efficiency from total input power to 852nm.

Feasibility of further scaling of the DRSFM output is seen from the simulation. With 10W of input power of 10W and at each wavelength, and 0.5% of passive loss of the resonator at each wavelength, $0.5 \times 10^{-4} \text{ W}^{-1}$ of normalized nonlinear efficiency, and $R=96\%$ at 1907nm and $R=98\%$ at 1540nm for the input coupler (same parameter as the experiment, with perfect mode matching), an output power of 13.2W with 66% conversion efficiency is expected, showing good scalability of the approach. The result of the simulation is shown in Figure 7.

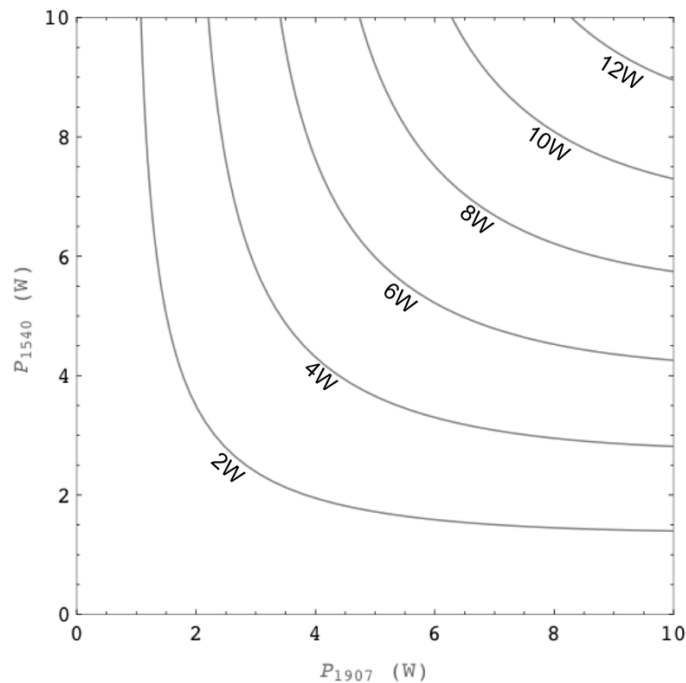


Figure 7. Contour plot of simulation of DRSFM output power at 852nm

The DRSFM cavity had to be sealed and dried, as the water vapor absorption at 1907nm severely affect the behavior of the resonance. Figure 8 shows the oscilloscope trace of the transmission signal from the cavity at 1907nm with the enclosure opened and sealed with desiccant for 40 minutes. In the cavity unit open to the environment, the transmission

peak at 1907nm shows substantial broadening while the PZT voltage is ramping down (cavity length is swept longer), indicating self-heating effect in the cavity with negative thermos-optic coefficient. Peak of 1540nm is not affected. We identified this as the moisture in the air. By detuning the temperature of the FBGs of the master oscillator, the significance of the broadening of the peak in the down-ramp could be reduced by a change in wavelength by less than 1nm, implying the absorption feature is sharp, likely from molecular source, and at the constant wavelength, the effect is dramatically reduced by sealing the cavity compartment with desiccant for more than half an hour. In a practical device, slightly different combination of the two wavelengths must be chosen and/or the DRSFM unit must be closed with clean dry air flow.

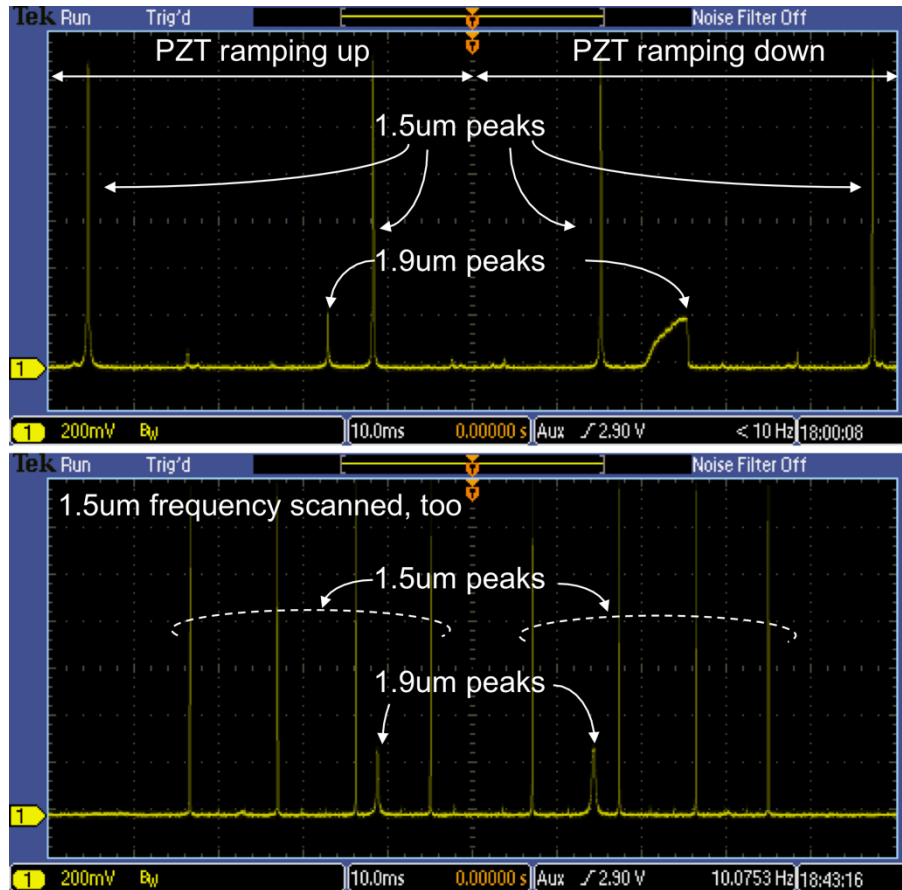


Figure 8. Oscilloscope screenshots of the DRSFM cavity transmission with cavity open to environment and 40 minutes after sealed with desiccant. The 1907nm transmission peak clearly changes in the down-ramp of the PZT.

4. HARMONIC GENERATION AT 213NM

With up to 4.02W of 852nm available for the harmonic generation, 2.41W of 426nm was obtained from the first external resonant doubler containing 20mm long type-I LBO cut at $\phi=90^\circ$, $\theta=27.4^\circ$ for the type-I critical phasematching at room temperature. The conversion efficiency is 60%.

For the harmonic generation at 213nm, BBO is practically the only choice as the nonlinear material. We used a Brewster-cut, 10mm long, Czochralski-grown BBO crystal cut at $\theta=72.9^\circ$ for the type-I phasematched SHG at 213nm [7]. The second resonant doubler consists of 3 high reflectors and an input coupler, and a dichroic Brewster beamsplitter; a fused silica plate with the angle of incidence of 56° with the first surface coated for high reflection at 213nm in s-polarization and high transmission at 426nm in p-polarization. Two of the high reflectors are concave with the radius of curvature of 100mm, and all other optical surfaces are flat. The resonator mode at 426nm has the waist of 44 μm (non-walkoff direction) and 35 μm (walkoff direction) in radius. We estimate the normalized conversion efficiency to be approximately $0.5 \times 10^{-4} \text{ W}^{-1}$.

With 2.41W at 426nm incident onto the second doubler, a maximum power of 0.456W at 213nm was observed. The conversion efficiency was 19%, after the 22% loss for the 213nm at the exit face of the BBO crystal. We estimate the circulating power in the doubler to be approximately 100W.

5. SUMMARY

We used 2 fiber amplifier sources at 1540nm and 1907nm and used DRSFM to efficiently generate 852nm in an external resonator. The maximum output power at 852nm was 5.2W. The operation of DRSFM was discussed. Using up to 4W of 852nm, we demonstrated the highest output power of CW 213nm reported so far, 0.456W, to the best of our knowledge. With the scalability of the fiber amplifier output, 852nm output power is also scalable, hence the CW output power at 213nm as well.

We gratefully acknowledge the support from New Energy and Industrial Technology Development Organization (NEDO) of Japan.

REFERENCES

- [1] J. Sakuma, Y. Asakawa, T. Imahoko, and M. Obara, "Generation of all-solid-state, high-power continuous-wave 213-nm light based on sum-frequency mixing in CsLiB₆O₁₀," *Opt. Lett.* **29**, 1096-1098 (2004).
- [2] Y. Kaneda, U.S. Patent 9,429,813 "Deep ultraviolet laser generation device and light source device," (2016).
- [3] D. Gapontsev, N. Platonov, M. Meleshkevich, O. Mishechkin, O. Shkurikhin, S. Agger, P. Varming, and J. H. Poylsen, "20W single-frequency fiber laser operating at 1.93 μ m," in *Conference on Lasers and Electro-Optics 2007*, paper CFI5 (2007).
- [4] Y. Jeong, J. K. Sahu, D. B. S. Soh, C. A. Codemard, and J. Nilsson, "High-power tunable single-frequency single-mode erbium:ytterbium codoped large-core fiber master-oscillator power amplifier source," *Opt. Lett.* **30**, 2997-2999 (2005).
- [5] Y. Kaneda, and S. Kubota, "Theoretical treatment, simulation, and experiments of doubly resonant sum-frequency mixing in an external resonator," *Appl. Opt.* **36**, 7766-7775 (1997).
- [6] C. Spiegelberg, J. Geng, Y. Hu, Y. Kaneda, S. Jiang, and N. Peyghambarian, "Low-noise narrow-linewidth fiber laser at 1550 nm (June 2003)," *IEEE J. Lightwave Technol.* **22**, 57-62 (2004).
- [7] K. Kato, N. Umemura, and T. Mikami, "Sellmeier and thermo-optic dispersion formulas for β -BaB₂O₄ (revisited)," *Proc. SPIE* **7582**, 75821L (2010).